

Free-standing 2D Nanorrafts by Assembly of 1D Nanorods for Biomolecule Sensing

Ren Cai,^{†,‡} Yaping Du,^{||} Dan Yang,[#] Guohua Jia,^Δ Bowen Zhu,[#] Bo Chen,[#] Yifan Lyu,^{†,‡} Kangfu Chen,^Φ Dechao Chen,^Δ Wei Chen,^Δ Lu Yang,[†] Yuliang Zhao,[◇] Zhuo Chen,[‡] and Weihong Tan,^{‡,‡,†*}

[‡]Molecular Science and Biomedicine Laboratory (MBL), State Key Laboratory for Chemo/Bio-Sensing and Chemometrics, College of Chemistry and Chemical Engineering, College of Biology, and Collaborative Research Center of Molecular Engineering for Theranostics, Hunan University, Changsha 410082, China

[‡]Institute of Molecular Medicine (IMM), Renji Hospital, Shanghai Jiao Tong University School of Medicine, and College of Chemistry and Chemical Engineering, Shanghai Jiao Tong University, Shanghai, China

[†]Center for Research at Bio/Nano Interface, Department of Chemistry and Department of Physiology and Functional Genomics, Shands Cancer Center, UF Genetics Institute and McKnight Brain Institute, University of Florida, Gainesville, Florida 32611-7200, United States

^{||}School of Material Science and Engineering, Nankai University, Tianjin 300350, China

^ΔNanochemistry Research Institute, Department of Chemistry, Curtin University, P.O. Box U1987, Perth, WA 6845, Australia.

[◇]National Center for Nanoscience and Technology, Chinese Academy of Sciences, Beijing 100049, China

[#]School of Materials Science and Engineering, Nanyang Technological University, 50 Nanyang Avenue, Singapore 639798, Singapore

^ΦDepartment of Mechanical and Aerospace Engineering, University of Florida, Gainesville, Florida 32611-6250, United States

* To whom correspondence should be addressed.

Email: tan@chem.ufl.edu

Experimental section

Chemicals

The following chemicals were used as obtained: oleic acid (OA, 90%, Sigma-Aldrich), 1-octadecene (OED, 90%, technical grade, Sigma-Aldrich), oleylamine (99%, Sigma-Aldrich), trifluoroacetic acid (CF_3COOH , 99%, Sigma-Aldrich), diethylene glycol (DEG, 99%, Sigma-Aldrich), dodecyl trimethylammonium bromide (DTAB, 99%, Sigma-Aldrich), magnesium trifluoroacetate (99%, Sigma-Aldrich), ammonium tungstate (99%, Sigma-Aldrich), copper (II) acetylacetonate ($\text{Cu}(\text{acac})_2$, 99.99%, Sigma-Aldrich), indium (III) acetylacetonate ($\text{In}(\text{acac})_3$, 99.99%, Sigma-Aldrich), zinc acetylacetonate ($\text{Zn}(\text{acac})_2$, 99.99%, Sigma-Aldrich), 1-dodecanethiol (1-DDT, >97%, Sigma-Aldrich), tert-dodecanethiol (t-DDT, 98.5%, mixture of isomers, Sigma-Aldrich), trioctylphosphine oxide (TOPO, 99%, Sigma-Aldrich), trioctylphosphine (TOP, 97%, Sigma-Aldrich), bis(trimethylsilylmethyl) sulfide ($(\text{TMS})_2\text{S}$, $\geq 98.0\%$, Sigma-Aldrich), tributylphosphine (TBP, 97%, Sigma-Aldrich), sulfur (S, 99%, Sigma-Aldrich), octadecylphosphonic acid (ODPA, 99%, Sigma-Aldrich), hexylphosphonic acid (HPA, 99%, Sigma-Aldrich), cadmium oxide (CdO , 99.5%, Sigma-Aldrich), octadecylamine (ODA 97%, Sigma-Aldrich), hexadecylamine (HAD, 98%, Sigma-Aldrich), hydroxylammonium chloride (99%, Sigma-Aldrich), ZnCl_2 (99.995%, Sigma-Aldrich), lithium triethylborohydride (1 M in tetrahydrofuran, Sigma-Aldrich), selenium powder (99.999%, Strem Chemicals), methanol (absolute for analysis, 99%, Sigma-Aldrich), chloroform, hexane, acetone and ethanol (absolute for analysis, ACS, 99.9%, Merck). All materials were used without further purification.

Synthesis of MgF_2 nanorods (NRs) (length = 110 ± 10 nm, width = 7 ± 1 nm): The following is a typical synthetic procedure for MgF_2 NRs. Magnesium trifluoroacetate (1.5 mmol) and 20 mmol oleic acid were dissolved in 20 mmol 1-octadecene at room temperature. The mixture was heated to 110°C and maintained for 30 min under Ar protection. The reaction mixture was heated to 300°C with a constant heating rate of $3.3^\circ\text{C min}^{-1}$ and then held 60 min. When the reaction temperature reached 300°C , an obvious reaction occurred, and the initially transparent solution became turbid. The colloidal solution was washed 3 times using ethanol/hexane (1:1 v/v) by sedimentation and redispersal using a centrifuge (5000 rpm for 10 min). Finally, the MgF_2 NRs were weighed and redispersed in hexane at

the desired NR concentration.

Synthesis of WO₂ NRs (length = 100±10 nm, width = 6±1 nm): The following is a typical synthetic procedure for WO₂ NRs. Ammonium tungstate (0.1 mmol) and 2 mmol oleic acid were dissolved in 18 mmol oleylamine at room temperature. The mixture was heated to 110 °C and maintained for 30 min under Ar protection. The reaction mixture was heated to 300 °C with a constant heating rate of 3.3 °C min⁻¹ and then held 30 min. When the reaction temperature reached 300 °C, an obvious reaction occurred, and the initially transparent solution became turbid. The colloidal solution was washed 3 times using ethanol/hexane (1:1 v/v) by sedimentation and redispersal using a centrifuge (5000 rpm for 10 min). Finally, the WO₂ NRs were weighed and redispersed in chloroform at the desired NR concentration.

Synthesis of CdS NRs (length = 67 ±6 nm, width = 4.3 ± 0.3 nm):¹ (I) Synthesis of CdS seeds, TOPO (3.299 g), ODPA (0.603 g) and CdO (0.100 g) were mixed in a 50 mL flask, heated to 150 °C and exposed to vacuum for 1 hour. Then, under nitrogen, the solution was heated to above 300 °C to dissolve the CdO until the solution turned optically clear and colorless. The temperature was stabilized at 320 °C and a mixture of (TMS)₂S (0.170g) and TBP (3g) was injected swiftly. The heat-controller was set to 250 °C and the nanocrystals were allowed to grow at this temperature for several minutes, depending on the final desired size. As an example, a reaction time of 7 min led to nanocrystals with an average diameter of 3.5 nm. After the synthesis, the nanocrystals were precipitated with methanol, then washed by repeated re-dissolution in toluene and precipitation with the addition of methanol, and they are finally dissolved in TOP.

(II) Synthesis of CdS NRs, TOPO (3 g), ODPA (0.29 g), HPA (0.080 g) and CdO (0.060 g) were mixed in a 50 mL flask, heated to 150 °C and exposed to vacuum for 1 hour. Then, under nitrogen, the solution was heated to above 380 °C to dissolve the CdO until it turned optically clear and colorless. At this step 1.5 g of TOP was injected, after which the temperature was allowed to recover to the value required for the injection of the solution of sulphur precursor + nanocrystals. Such solution is prepared by dissolving S (0.120 g) in TOP and adding to this 200 µL of a solution of readily prepared CdS dots dissolved in TOP (the concentration of dots in the TOP solution was always 400 µM). As an example, a reaction time of 7 min led to nanocrystals with an average diameter of 3.5 nm. After the synthesis, the

nanocrystals were precipitated with methanol, then washed by repeated re-dissolution in toluene and precipitation with the addition of methanol, and they were finally dissolved in TOP. The resulting solution was quickly injected in the flask. After injection, the temperature dropped to 270-300°C and it recovered within two minutes to the pre-injection temperature. The nanocrystals were allowed to grow for about 8 minutes after the injection, after which the heating mantle was removed. The colloidal solution was washed 3 times using ethanol /hexane (1:1 v/v) by sedimentation and redispersal using a centrifuge (5000 rpm for 5 min). Finally, the CdS NRs were weighed and redispersed in hexane at the desired nanorod concentration.

Synthesis of ZnS NRs (length = 120 ± 15 nm, width = 3.5 ± 0.3 nm):² (I) Synthesis of ZnS nanowires: 0.05 mmol (18 mg) of zinc diethyldithiocarbamate and 10 mL of oleylamine were mixed in a three-necked flask. The mixture was degassed and refilled with Ar three times at room temperature and then heated to 110 °C and kept at this temperature for 0.5 h. Then the temperature was raised from 110 to 230 °C in 6 min. After 20 min at 230 °C, the reaction was quenched by removing the heating mantle.

(II) Purification of Zinc chalcogenide nanowires: the crude zinc chalcogenide nanowire product solution was dissolved in chloroform, and the nanowires were precipitated by adding methanol with the aid of centrifugation.

(III) Aging of ZnS nanowires: After purification, ZnS nanowires were redissolved in oleylamine, and then the reaction solution was kept in the glovebox at room temperature for 2~4 weeks prior to the synthesis of ZnS quantum nanorods.

(iv) Synthesis of ZnS NRs: Purified zinc chalcogenide nanowires were re-dissolved in oleylamine in a three-necked flask. The reaction mixture was degassed and refilled with Ar three times at room temperature and then heated to 110 °C and kept at this temperature for 10 min. Then the reaction solution was heated to 280 °C in 10 min and kept at this temperature for 30 min. The reaction was terminated by removing the heating mantle.

Synthesis of ZnSe NRs (length = 115 ± 17 nm, width = 3.6 ± 0.3 nm):² (I) Synthesis of ZnSe nanowires: 0.2 mmol (59.5 mg) of Zn(NO₃)₂·6H₂O and 30 mL of oleylamine were mixed in a three-

necked flask. The mixture was degassed and refilled with Ar three times at room temperature and then heated to 110 °C and kept at this temperature for 0.5 h. The mixture was then heated to 160 °C, and 2 mL of a 0.1 M solution of Se in oleylamine was injected into the flask. After the injection, the temperature was set at 120 °C, and the mixture was degassed for 10 min. Then the temperature was raised to 230 °C in 6 min. After 20 min at 230 °C, the reaction was quenched by removing the heating mantle.

(II) Purification of Zinc chalcogenide nanowires: the crude zinc chalcogenide nanowire product solution was dissolved in chloroform, and the nanowires were precipitated by adding methanol with the aid of centrifugation.

(III) Aging of ZnSe nanowires: After purification, ZnSe nanowires were re-dissolved in oleylamine, and then the reaction solution was kept in the glovebox at room temperature for 2~4 weeks prior to the synthesis of ZnSe quantum nanorods.

(iv) Synthesis of ZnSe NRs: Purified zinc chalcogenide nanowires were re-dissolved in oleylamine in a three-necked flask. The reaction mixture was degassed and refilled with Ar three times at room temperature and then heated to 110 °C and kept at this temperature for 10 min. Then the reaction solution was heated to 280 °C in 10 min and kept at this temperature for 15 min. The reaction was terminated by removing the heating mantle.

Synthesis of 2D nanorrafts from WO₂ NRs: In a typical self-assembly experiment, 40 μL 1-octadecene (ODE) was added to a chloroform solution of WO₂ NRs (1 mg, 400 μL) by a vortex mixer for 30 min. The remaining experimental steps were the same as those for the synthesis of 2D MgF₂ nanorrafts.

Synthesis of 2D nanorrafts from CdS NRs: In a typical self-assembly experiment, 20 μL 1-octadecene (ODE) was added to a hexane solution of CdS NRs (1 mg, 500 μL) by a vortex mixer for 30 min. The remaining experimental steps were same as those for the synthesis of 2D MgF₂ nanorrafts.

Synthesis of 2D nanorrafts from ZnS NRs: In a typical self-assembly experiment, 20 μL 1-octadecene (ODE) was added to a hexane solution of ZnS NRs (1 mg, 500 μL) by a vortex mixer for 30 min. The remaining experimental steps were same as those for the synthesis of 2D MgF₂ nanorrafts.

Synthesis of 2D nanorrafts from ZnSe NRs: In a typical self-assembly experiment, 20 μL 1-octadecene (ODE) was added to a hexane solution of ZnSe NRs (1 mg, 500 μL) by a vortex mixer for 30 min. The remaining experimental steps were same as those for the synthesis of 2D MgF_2 nanorrafts.

Materials Characterization

Morphology of the samples was characterized with a transmission electron microscope (TEM) system (JEOL Model JEM-2010F) operating at 200 kV. UV-Vis measurements were performed with a Cary Bio-100 UV/Vis spectrometer (Varian). Atomic force microscopy (AFM) (Digital Instruments) was used to determine the thickness of the nanorrafts. NMR spectra were recorded on a Varian Unity spectrometer (400 MHz for ^1H NMR). All spectra were examined using MestReNova 8.1 (Mnova) software and displayed without the use of the signal suppression function. The crystal phase of samples was investigated using a Bruker D8 Advance diffractometer X-ray diffraction (XRD) at the 2θ range of 10° to 80° with $\text{Cu K}\alpha$ radiation. Fluorescence emission spectral measurements were performed with a Fluorescence Spectroscopy of HORIBA Jobin Yvon.

The energy or entropy analysis of self-assembled mechanism of 2D nanorods:

As we known, entropy-driven self-assembled formation is the one that minimize the system free energy (Helmholtz free energy, F), expressed in terms of energetic (U) and entropic (S) components as³

$$F = U - TS. \quad (1-1)$$

The free energy change ΔF upon self-assembly provides the driving force for ordering and results from corresponding changes in system internal energy and entropy,

$$\Delta F = \Delta U - T\Delta S. \quad (1-2)$$

Usually, the internal energy change of the assembling system would be broken down approximately into core (e.g., building block) and ligand contributions,⁴

$$\Delta U \approx \delta U_{cores} + \delta U_{ligands}, \quad (1-3)$$

as can be entropy,

$$\Delta S \approx \delta S_{cores} + \delta S_{ligands}. \quad (1-4)$$

Energetic interactions between cores (i.e., building block (MgF₂ NRs)) are described by the set of van der Waals interactions,⁵

$$\delta U_{cores} \approx \delta U_{vdW} \approx \delta U_{London} + \delta U_{Keesom} + \delta U_{Debye}. \quad (1-5)$$

δU_{London} : London dispersion attraction; δU_{Keesom} : dipole-induced dipole interactions; δU_{Debye} : dipole-dipole interactions. Here, London dispersion force is the weakest intermolecular force. For hard core- MgF₂ NRs, $\delta U_{London} \approx 0$. This elastic resistance to chain (ligands) deformation balances the attractive London dispersion interaction between aliphatic chains (e.g., 1-octadecene (ODE)): ⁶

$$\delta U_{ligands} \approx \delta U_{elastic} + \delta U_{London} \approx \delta U_{elastic} + 0 \approx \delta U_{elastic}. \quad (1-6)$$

Meanwhile, core (building block) entropy has configurational, translational, and rotational terms,⁷

$$\delta S_{cores} \approx \delta S_{conf} + \delta S_{trans} + \delta S_{rot}. \quad (1-7)$$

In our assembly system, nanorod is hard (building block) cores, the configurational, translational, and rotational rearrangement of the nanorods in the system would be ignoring local effects, i.e.

$$\delta S_{cores} \approx \delta S_{conf} + \delta S_{trans} + \delta S_{rot} \approx 0 \quad (1-7)$$

Here, used (1-3), (1-4), (1-5), (1-6) and (1-7) into (1-2):

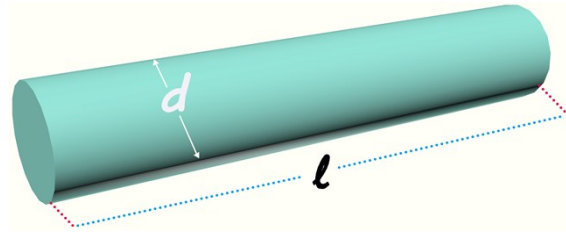
$$\begin{aligned} \Delta F &= \Delta U - T\Delta S \approx (\delta U_{cores} + \delta U_{ligands}) - T(\delta S_{cores} + \delta S_{ligands}), \\ &\approx (\delta U_{vdW} + (\delta U_{elastic} + \delta U_{London})) - T(0 + \delta S_{ligands}) \\ &\approx \delta U_{vdW} + (\delta U_{elastic} + \delta U_{London}) - T\delta S_{ligands} \approx \delta U_{vdW} + \delta U_{ligands} - T\delta S_{ligands} \end{aligned} \quad (1-8)$$

$$\text{In sum, } \Delta F \approx \delta U_{vdW} + \Delta F_{ligands} \quad (1-8)$$

$$\Delta F_{ligands} \approx \delta U_{ligands} - T\delta S_{ligands} \approx \delta U_{elastic} + 0 - T\delta S_{ligands} \approx \delta U_{elastic} - T\delta S_{ligands} \quad (1-9)$$

Therefore, in the formation of 2D nanorrafts, there is a balance of the elastic repulsive force ($\Delta F_{ligands} \approx \delta U_{elastic} - T\delta S_{ligands}$) contributed by the ligands (ODE) and van der Waals attractive forces (δU_{vdW}).^{8,9,10}

Calculation of the number of nanorods (NRs) ($N_{nanorods}$)



For one nanorod, the average radius is r . The density, mass and volume are ρ , m_1 and V_1 . The mass of one nanorod (m_1) was calculated as

$$m_1 = \rho \cdot V_1 \quad (1)$$

$$V_1 = \pi r^2 \cdot l \quad (2)$$

$$m_1 = \rho \cdot V_1 = \rho \cdot \pi r^2 l \quad (3)$$

The number of nanorods ($N_{nanorods}$) was calculated as

$$N_{nanorods} = \frac{m_{Total}}{m_1} = \frac{m_{Total}}{\rho \cdot V_1} = \frac{m_{Total}}{\rho \cdot \pi r^2 l} \quad (4)$$

where $\rho=3.148 \text{ g/cm}^3$, $d=2r=6\pm0.5 \text{ nm}$, $l=105\pm10 \text{ nm}$, and m_{Total} is the total mass that was weighed in the experiment: $m_{Total}=1 \text{ mg}$ and $N_{nanorods}=(1.071\pm0.205) \times 10^{14}$ in 1 mg total mass.

Calculation of the number of 1-octadecene (ODE) molecules (N_{ODE})

For ODE molecules, N_A is Avogadro's number ($N_A=6.022 \times 10^{23} \text{ mol}^{-1}$), n is the number of moles, M_{ODE} is the molecular weight, and m is total mass. The number of ODE molecules (N_{OA}) was calculated as

$$N_{ODE} = n \cdot N_A \quad (5)$$

$$n = \frac{m}{M_{ODE}} \quad (6)$$

$$m = \rho \cdot V \quad (7)$$

The number of ODE molecules (N_{ODE}) was calculated as

$$N_{ODE} = n \cdot N_A = \frac{m}{M_{ODE}} \cdot N_A = \frac{\rho \cdot V}{M_{ODE}} \cdot N_A \quad (8)$$

where $\rho=0.789$ g/cm³, $M_{ODE}= 252.48$ g/mol, and the OED content of the purchased material was 90% (OED, 90%, technical grade, Sigma-Aldrich).

Calculation of the number of ODE molecules per nanorod (N_0)

$$N_0 = \frac{N_{ODE}}{N_{nanorods}}$$

The N_{ODE} and N_0 were calculated as follows:

V_{ODE}	N_{ODE}	N_0
0 μ L	0	0
5 μ L	8.469 x 10 ¹⁸	7.907 x 10 ⁴
15 μ L	2.541 x 10 ¹⁹	2.372 x 10 ⁵
20 μ L	3.388 x 10 ¹⁹	3.163 x 10 ⁵
30 μ L	5.081 x 10 ¹⁹	4.744 x 10 ⁵

These data were used to prepare **Figure S7**.

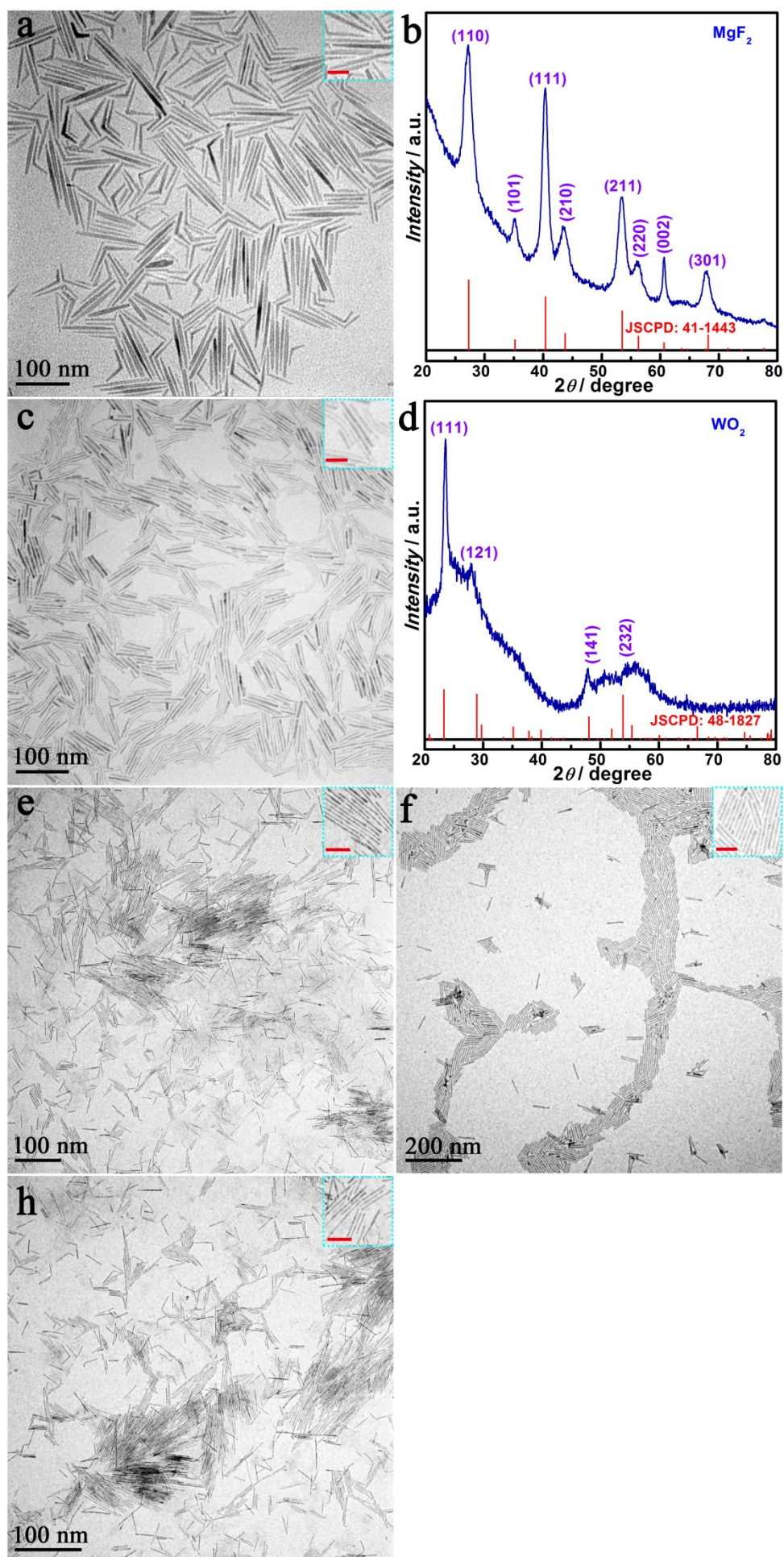


Figure S1 TEM images of NR building blocks: a) MgF₂ NRs and b) XRD; c) WO₂ NRs and d) XRD; e) ZnS NRs; f) CdS NRs; h) ZnSe NRs. The scales bars are 20 nm in inset images.

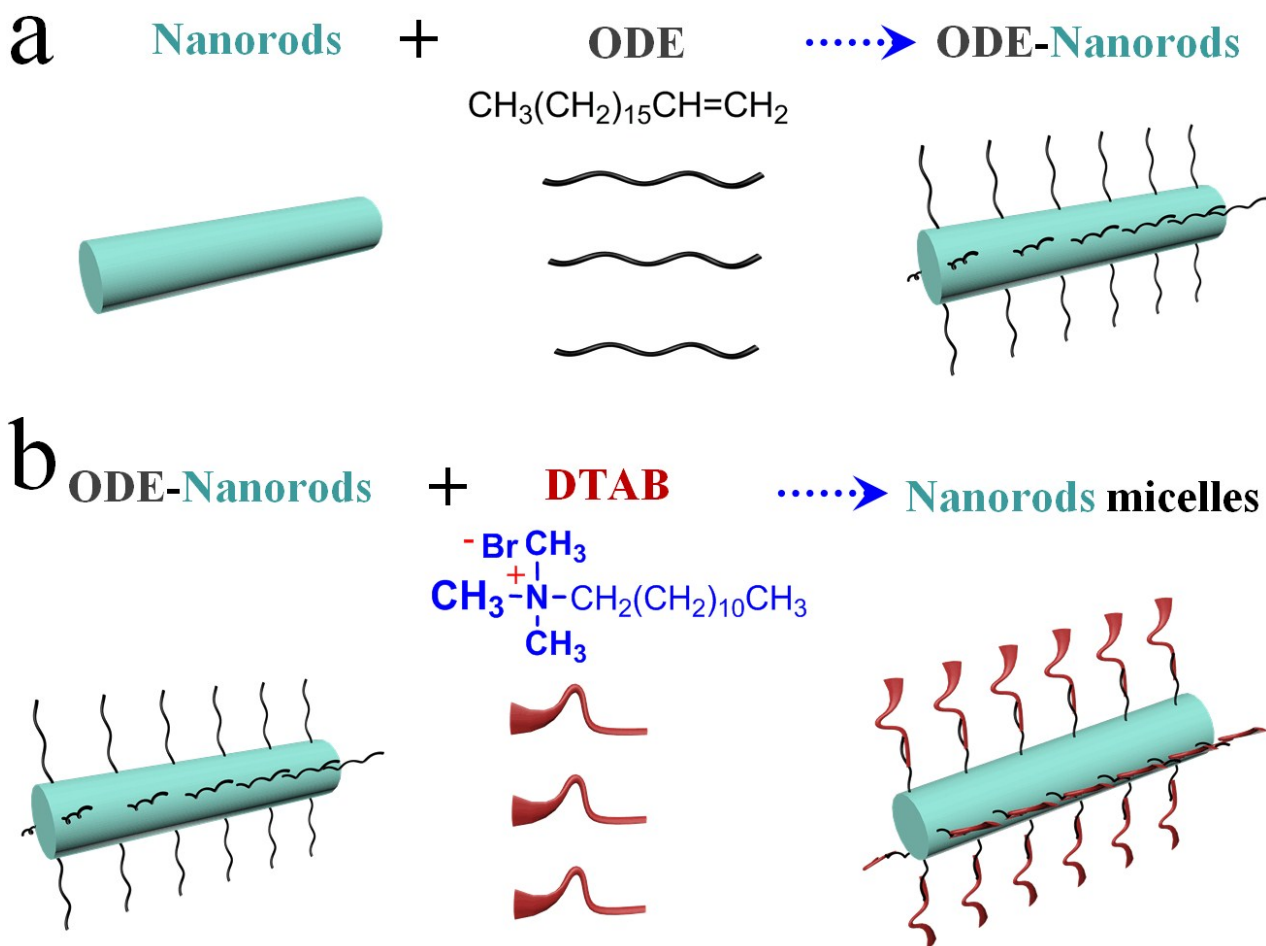


Figure S2 Scheme for the formation of NR micelles: a) ODE-capped NRs; b) NR micelles.

Note: These micelles were synthesized as follows: An aqueous solution of DTAB was added to ODE-capped NRs (ODE-NRs, **Figure S2a**) in hexane and heated to create a water-in-oil microemulsion (**Figure S2b**). DTAB, a cationic surfactant, was used to transfer ODE-capped NRs to hydrophilic solution by a ligand-wrapped reaction,¹¹ forming an interdigitated bilayer structure (**Figure S2b**).¹² After injection of mixed solvent (DEG and PVP), some NR micelles were quickly encapsulated by mixed solvent (PVP in DEG), which is a protective layer to stabilize these capping micelles from repulsive steric interactions (**Figure 3a**).¹³ During the thermal-annealing process (83 °C, 2.5 h), hexane evaporated from the system, and the DTAB layer (secondary layer, **Figure S2b**) detached from the surface of NR micelles because of good solubility of DTAB in DEG.¹⁴ This led to micelle decomposition to reform ODE-NRs (**Figure 3b**). Finally, ligand elastic repulsion contributed by the ligands (ODE)¹⁵ and stronger van der Waals attractive forces among ODE-NRs were all induced, leading to NR assembly with the help of the annealing process (**Figure 3c**).¹⁶

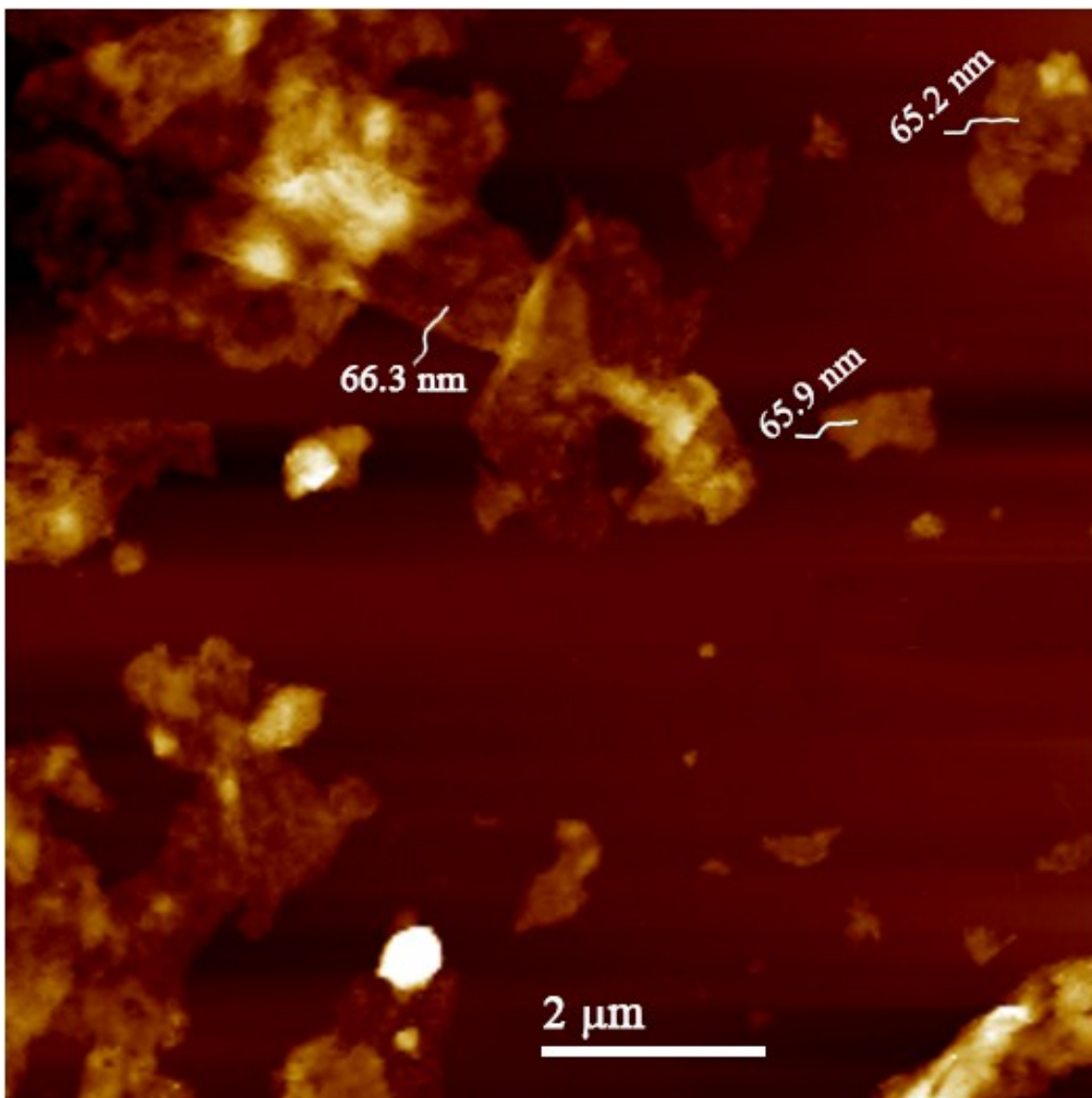


Figure S3 AFM images of MgF₂ nanorrafts.

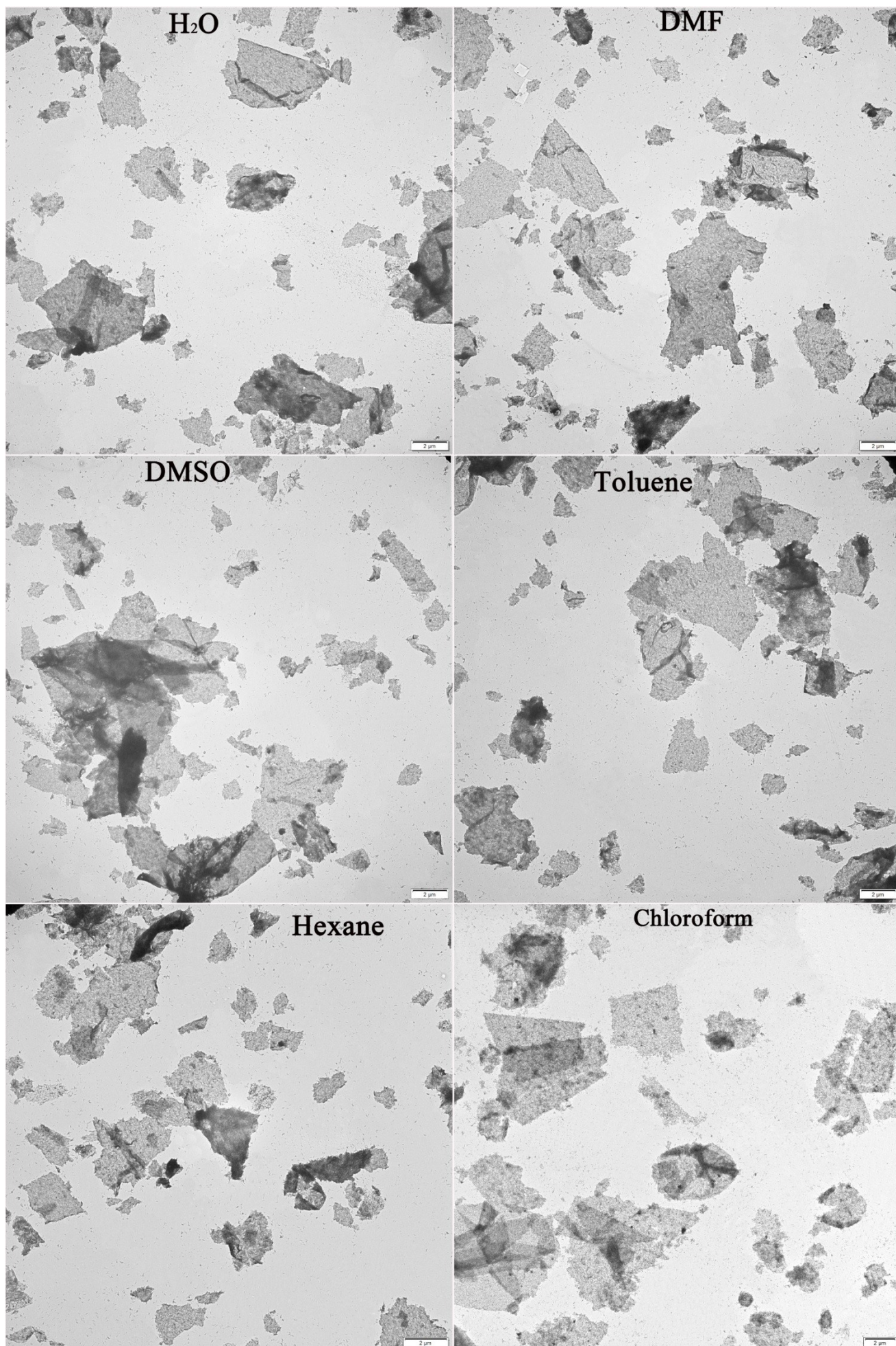


Figure S4 The TEM images of 2D nanorrafts after they were stored in different solvents for 24 hours: (DI-water; dimethylformamide (DMF); dimethyl sulfoxide (DMSO); toluene; hexane; chloroform).

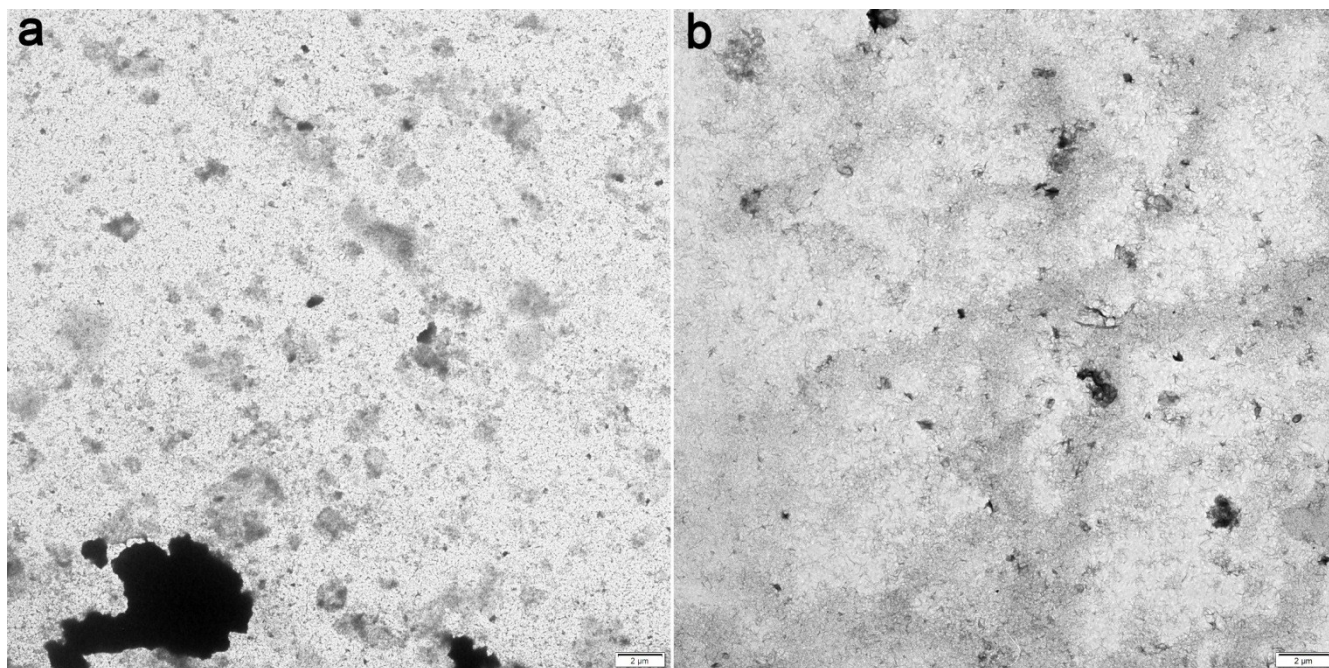


Figure S5 Samples prepared from the assembly of 1D NRs: a) without DTAB; b) without PVP.

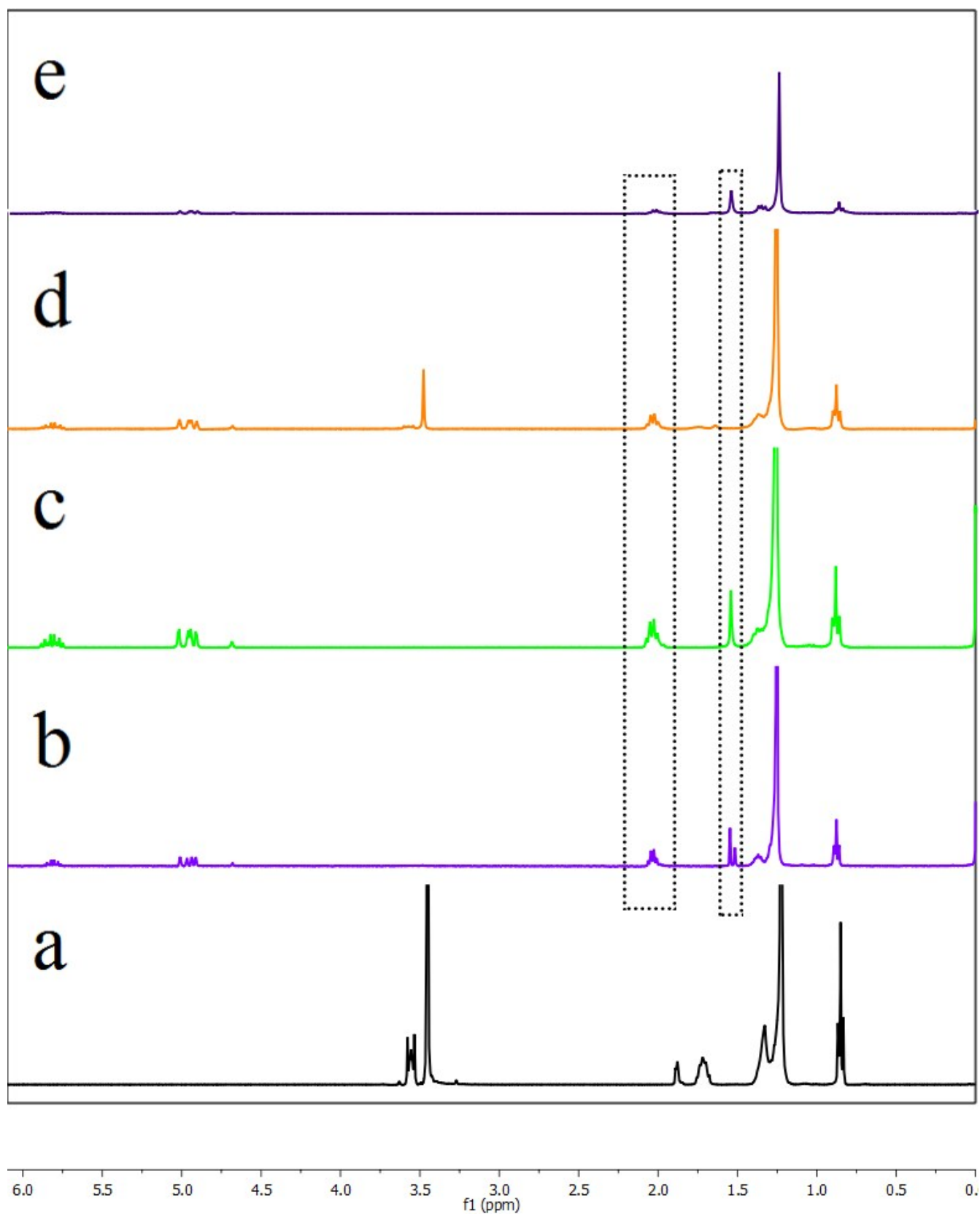


Figure S6 ¹H NMR spectra of a) DTAB, b) ODE, c) ODE-capped NRs, d) NR micelles (DTAB and ODE capped on the NRs), and e) the residual organic ligands (ODE) on the 2D nanorrafts (¹H NMR of nanorrafts was performed after HCl was used to slightly dissolve their surfaces).

Note: ¹H NMR spectra show that the organic ligands on the surface of NR micelles were both ODE and DTAB molecules in **Figure S6d**. In contrast, the residual organic ligands on the surface of nanorrafts were only ODE, while DTAB was not measurable in **Figure S6e**. These ¹H NMR results confirmed the loss of DTAB and presence of ODE during the assembly process.

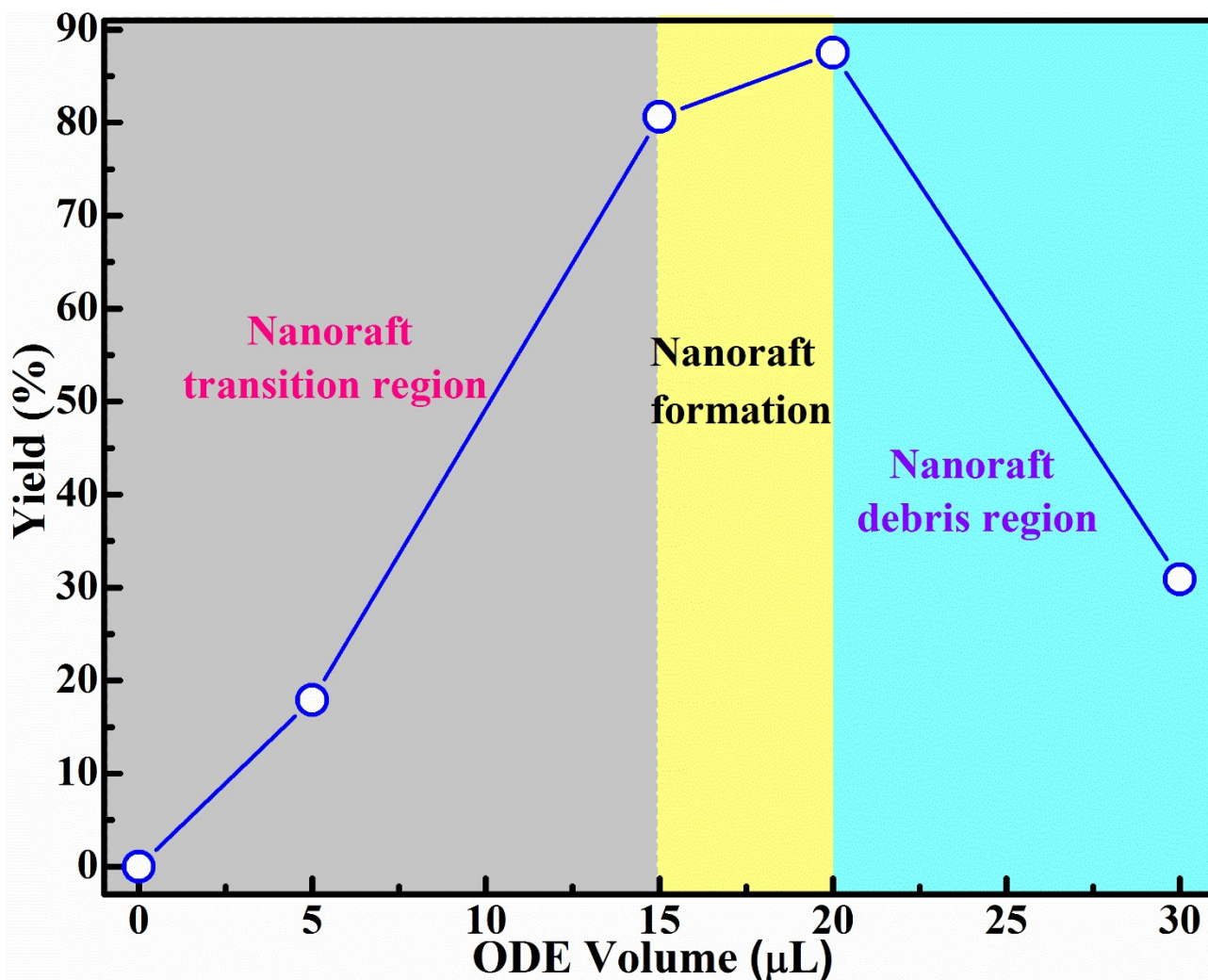


Figure S7 Relationship between the yield of 2D nanorafts and ODE volume.

References:

1. Carbone, L.; Nobile, C.; De Giorgi, M.; Sala, F. D.; Morello, G.; Pompa, P.; Hytch, M.; Snoeck, E.; Fiore, A.; Franchini, I. R.; Nadasan, M.; Silvestre, A. F.; Chiodo, L.; Kudera, S.; Cingolani, R.; Krahn, R.; Manna, L., Synthesis and Micrometer-Scale Assembly of Colloidal CdSe/CdS Nanorods Prepared by a Seeded Growth Approach. *Nano Lett.* **2007**, *7*, 2942-2950.
2. Jia, G.; Banin, U., A General Strategy for Synthesizing Colloidal Semiconductor Zinc Chalcogenide Quantum Rods. *J. Am. Chem. Soc.* **2014**, *136*, 11121-11127.

3. Boles, M. A.; Engel, M.; Talapin, D. V., Self-Assembly of Colloidal Nanocrystals: From Intricate Structures to Functional Materials. *Chem. Rev.* **2016**, *116*, 11220-11289.
4. Vogel, N.; Retsch, M.; Fustin, C. A.; del Campo, A.; Jonas, U., Advances in Colloidal Assembly: The Design of Structure and Hierarchy in Two and Three Dimensions. *Chem. Rev.* **2015**, *115*, 6265-6311.
5. Ohara, P. C.; Leff, D. V.; Heath, J. R.; Gelbart, W. M., Crystallization of Opals from Polydisperse Nanoparticles. *Phys. Rev. Lett.* **1995**, *75*, 3466-3469.
6. Saunders, A. E.; Korgel, B. A., Second Virial Coefficient Measurements of Dilute Gold Nanocrystal Dispersions Using Small-Angle X-ray Scattering. *J. Phys. Chem. B* **2004**, *108*, 16732-16738.
7. Shevchenko, E. V.; Talapin, D. V.; Kotov, N. A.; O'Brien, S.; Murray, C. B., Structural diversity in binary nanoparticle superlattices. *Nature* **2006**, *439*, 55.
8. Jenkins, P.; Snowden, M., Depletion flocculation in colloidal dispersions. *Adv. Colloid Interface Sci.* **1996**, *68*, 57-96.
9. Asakura, S.; Oosawa, F., On Interaction between Two Bodies Immersed in a Solution of Macromolecules. *J. Chem. Phys.* **1954**, *22*, 1255-1256.
10. Young, K. L.; Jones, M. R.; Zhang, J.; Macfarlane, R. J.; Esquivel-Sirvent, R.; Nap, R. J.; Wu, J.; Schatz, G. C.; Lee, B.; Mirkin, C. A., Assembly of reconfigurable one-dimensional colloidal superlattices due to a synergy of fundamental nanoscale forces. *Proc. Natl. Acad. Sci. U.S.A.* **2012**, *109*, 2240-2245.
11. Du, Y.; Yin, Z.; Zhu, J.; Huang, X.; Wu, X.-J.; Zeng, Z.; Yan, Q.; Zhang, H., A general method for the large-scale synthesis of uniform ultrathin metal sulphide nanocrystals. *Nat. Commun.* **2012**, *3*, 1177.
12. Fan, H.; Leve, E.; Gabaldon, J.; Wright, A.; Haddad, R. E.; Brinker, C. J., Ordered Two- and Three-Dimensional Arrays Self-Assembled from Water-Soluble Nanocrystal-Micelles. *Adv. Mater.* **2005**, *17*, 2587-2590.
13. Shahmiri, M.; Ibrahim, N. A.; Shayesteh, F.; Asim, N.; Motallebi, N., Preparation of PVP-coated copper oxide nanosheets as antibacterial and antifungal agents. *J. Mater. Res.* **2013**, *28*, 3109-3118.
14. Zhu, M.-Q.; Wang, L.-Q.; Exarhos, G. J.; Li, A. D. Q., Thermosensitive Gold Nanoparticles. *J. Am. Chem. Soc.* **2004**, *126*, 2656-2657.
15. Rabani, E.; Egorov, S. A., Solvophobic and Solvophilic Effects on the Potential of Mean Force between Two Nanoparticles in Binary Mixtures. *Nano Lett* **2002**, *2*, 69-72.
16. Min, Y.; Akbulut, M.; Kristiansen, K.; Golan, Y.; Israelachvili, J., The role of interparticle and external forces in nanoparticle assembly. *Nat. Mater.* **2008**, *7*, 527-538.